Phase diagram for morphological transitions of wetting films on chemically structured substrates

C. Bauer and S. Dietrich
Fachbereich Physik, Bergische Universität Wuppertal, D-42097 Wuppertal, Germany
(Received 19 August 1999)

Using an interface displacement model we calculate the shapes of thin liquidlike films adsorbed on flat substrates containing a chemical stripe. We determine the entire phase diagram of morphological phase transitions in these films as function of temperature, undersaturation, and stripe width.

PACS number(s): 68.45.Gd, 68.10.−m, 82.65.Dp

I. INTRODUCTION

At present various experimental techniques allow one to provide substrates with well-defined, microscopically small geometrical or chemical structures or combinations thereof (see, e.g., Ref. [1]). These structured substrates can serve as devices to guide and process tiny amounts of liquids. Such ''microfluidics'' systems [2] are promising for future applications, e.g., in chemistry and biology [3,4]. Although the performance of these systems ultimately depends on their dynamic properties, a thorough understanding of the corresponding structural properties in thermal equilibrium is an important prerequisite [5]. In this spirit as a paradigmatic case we determine the equilibrium structures of liquidlike wetting films forming at the interface between a bulk vapor phase and a flat solid substrate containing a single chemical stripe (Fig. 1). Our aim is to explore the entire phase diagram for the emerging lateral fluid structures as function of temperature, undersaturation or pressure, and stripe width.

In Ref. [6] it has been shown that a thin liquidlike film adsorbed on such a substrate (Fig. 1) can undergo an interesting morphological phase transition (Figs. 2 and 3) of the shape $l(x)$ of the liquid-vapor interface, depending on the structures of the effective interface potentials $\Lambda_{\pm}(l)$ characterizing the corresponding *homogeneous* substrates ''+'' and ''−'' (see, e.g., Fig. 4). In accordance with Ref. [6] we study a substrate designed such that the effective interface potential $\Lambda_{+}(l)$ of the stripe part exhibits two competing local minima (''I'' near and ''III'' further away from the substrate surface) whereas the asymptotic film thickness l_{-} far from the stripe is given by the single global minimum (''II'') of the interface potential $\Lambda_{-}(l)$ of the embedding substrate (see Fig. 4). In Ref. [6] the phase diagram for this morphological phase transition has been determined, at constant temperature T, as a function of the stripe width a and of the undersaturation $\Delta\mu=\mu_0-\mu\geqslant 0$ where $\mu_0(T)$ is the chemical potential at liquid-vapor coexistence. The purpose of the present study is to determine how this phase diagram for the morphological phase transition within the a-$\Delta\mu$ plane evolves as a function of temperature. This additional information is important in order to be able to put the morphological phase transitions into the context of T-$\Delta\mu$ wetting phase diagrams, including the prewetting line, on homogeneous substrates [7].

We emphasize that experimental techniques such as reflection interference contrast microscopy (RICM) [8] and atomic force microscopy (AFM) in tapping mode [9] are capable of imaging the liquidlike structures under consideration down to the nm scale. Moreover, due to their relatively small spatial extensions the structures discussed here are well accessible by Monte Carlo simulations as another means for testing the theoretical predictions. For these envisaged studies the knowledge of the full topology of the phase diagram as a function of T, $\Delta\mu$, and a is very important.

II. THEORETICAL MODEL

We use the following simple interface displacement model within which the equilibrium interface profile $\overline{l}(x)$ minimizes the functional:

$$\Omega_S[l(x)]=\int_A dx\,dy\,\Lambda(x,l(x))+\sigma_{lg}\int_A dx\,dy\left(\frac{dl(x)}{dx}\right)^2, \tag{1}$$

where $A=L_xL_y$ is the area of the flat substrate surface located at $z=0$. The first part takes into account the effective interaction between the liquid-vapor interface and the substrate via the laterally varying effective interface potential $\Lambda(x,l)=\Delta\Omega_b l+\omega(x,l)$. The second part in Eq. (1) is the leading-order term of a gradient expansion of the surface free energy associated with the deviation of the liquid-vapor in-

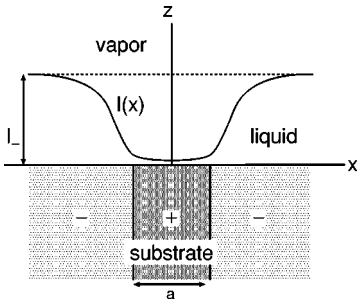

FIG. 1. Schematic cross section of the morphology of a liquidlike film covering a planar substrate which contains a slab of different material. In the top view the substrate forms a stripe composed of ''+'' particles extending from $x=-a/2$ to $x=a/2$. The substrate is translationally invariant in the y direction, with its surface located at $z=0$. $l_{-}=l(|x|\to\infty)$ is the equilibrium film thickness corresponding to a homogeneous substrate composed of ''−'' particles. The stripe (embedding) part exerts an effective interface potential $\Lambda_{+}(\Lambda_{-})$ on the liquid-vapor interface at the vertical distance $z=l(x)$. In the case shown here the − substrate prefers a thicker wetting film than the + substrate.

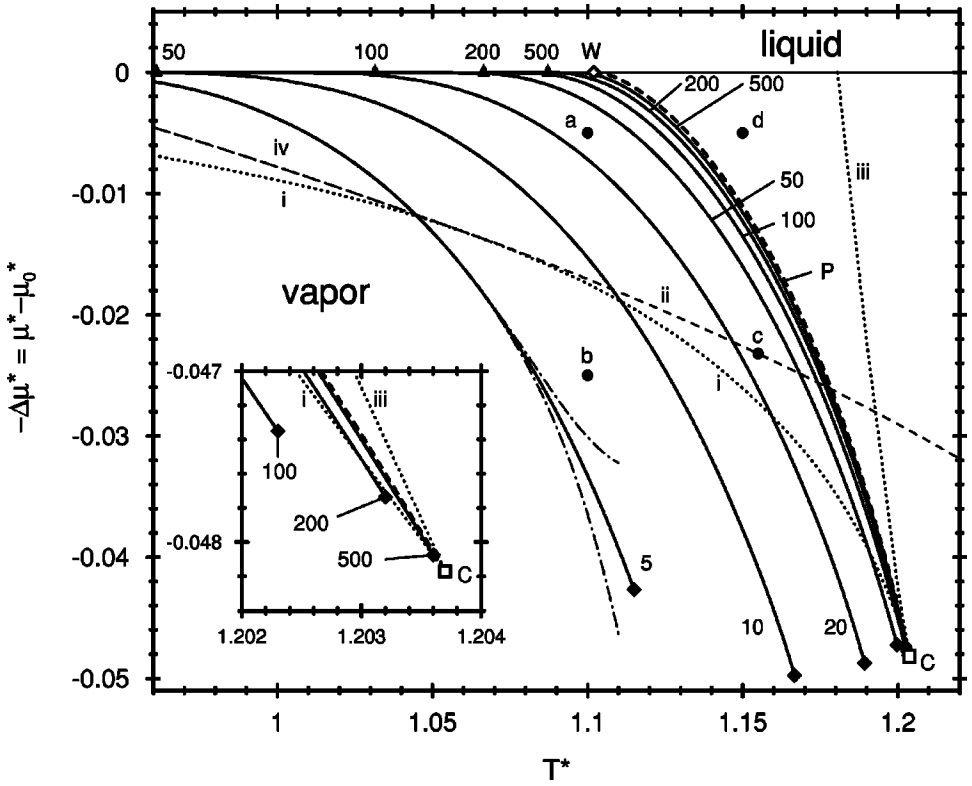

FIG. 2. T-$\Delta\mu$ phase diagram for the morphological transitions of a liquidlike layer on a chemical stripe (compare Fig. 1); $T^*=k_BT/\epsilon$ and $\mu^*=\mu/\epsilon$. $\Delta\mu=0$ is the bulk liquid-vapor coexistence line. For the present model the bulk critical temperature is $T_c^*\approx 1.412$; the estimated triple point temperature is $T_t^*\approx 0.8$. The *homogeneous* substrate composed of ''+'' particles, i.e., corresponding to the stripe, supports a first-order wetting transition at coexistence denoted by ''W'' ($\diamond$). The corresponding prewetting line ''P'' (thick dashed line) is attached tangentially and ends at a prewetting critical point ''C'' ($\square$). The effective interface potentials $\Lambda_{\pm}$ and, as examples, the equilibrium interface profiles at the thermodynamic states $\bullet$ denoted as ''a,'' ''b,'' ''c,'' and ''d'' are shown in Figs. 4–7 for $a/\sigma\approx 27.5,6.4,26$, and $a/\sigma=50$, respectively. For ''a,'' ''b,'' and ''c'' these values for the width a are those for which in these thermodynamic states the morphological phase transition takes place. The coexistence lines $\Delta\mu_t(T;a)$ (full lines) of the bound and the repelled solutions for fixed stripe width a are accompanied by the appertaining value a/σ. For $-\Delta\mu>-\Delta\mu_t$ the repelled solution and for $-\Delta\mu<-\Delta\mu_t$ the bound solution is the stable one. The lines of coexistence intersect the axis $\Delta\mu=0$ at the points $T_0(a)$ marked as $\blacktriangle$. $\Delta\mu_t(T;a)$ joins the bulk liquid-vapor coexistence curve tangentially with $\Delta\mu_t(T\rightarrow T_0(a);a)\sim(T-T_0(a))^{\delta}$; the numerical data indicate that δ is larger than the corresponding exponent $\delta=3/2$ for the prewetting line. Due to this tangential behavior the intersections $T_0(a)$ occur at lower temperatures than expected visually on the present scale. Therefore we have separately labeled the intersections $T_0(a)$ by the corresponding values for a/σ. All lines of coexistence end at a critical point denoted by $\blacklozenge$. The dash-dotted lines accompanying the line for $a=5\sigma$ show the region within which the fluctuation-induced rounding of the first-order phase transition takes place; for $a\geqslant 10\sigma$ this rounding effect is not visible on the present scale. The inset magnifies the region around the prewetting critical point ''C.'' The meaning of the lines ''i,'' ''ii,'' ''iii,'' and ''iv'' is discussed in the main text.

terface profile from its flat configuration; σ_{lg} is the surface tension. $\Delta\Omega_b=\Delta\mu(\rho_l-\rho_g)+O((\Delta\mu)^2)$ is the difference of the bulk free energy densities of the liquid and the vapor phase with number densities ρ_l and ρ_g, respectively. Alternatively, in terms of the bulk pressure p, $\Delta\Omega_b$ is given approximately by the Gibbs-Thomson expression $k_BT\rho_l\ln(p_{sat}/p)$ where p_{sat} is the saturated vapor pressure. At liquid-vapor coexistence $\Lambda(x,l)$ is given by $\omega(x,l)$ which is of the form $\Sigma_{i\geqslant 2}a_i(x)/l^i$. Since the substrate is translationally invariant in the y direction the effective interface potential depends only on x, so that $\overline{l}(x)$ is also translationally invariant in the y direction. For reasons of simplicity we assume that the lateral variation of $\omega(x,l)$ is steplike: $\omega(x,l)=\Theta(|x|-a/2)\omega_-(l)+\Theta(a/2-|x|)\omega_+(l)$ with the effective interface potential $\omega_+(\omega_-)$ of a *homogeneous* substrate composed of ''+'' (''−'') particles. In Refs. [10] and [11] we have shown that the functional in Eq. (1)—despite its simplicity—allows one to determine reliably the morphology of liquidlike films on structured substrates, and we have presented a derivation of this square-gradient functional from a microscopic density functional theory. We also found (see Fig. 11 in Ref. [10]) that the aforementioned steplike variation of $\omega(x,l)$ as opposed to its actual smooth lateral variation represents a rather reliable approximation. The form of $\omega(x,l)$ follows from considering as the interaction potential between the fluid particles a Lennard-Jones potential with a depth $-\epsilon$ and an effective particle diameter σ. Moreover, also the interaction between the fluid and the substrate particles is modeled by a Lennard-Jones potential. The interaction potential $V_{\pm}(z)=\Sigma_{i\geqslant 3}u_i^{\pm}/z^i$ between a homogeneous, flat ''+'' or ''−'' substrate and a fluid particle at a distance z follows from pairwise summation over all substrate-fluid particle interactions. As extensively discussed in Refs. [7,10,11], density functional theory provides a procedure to

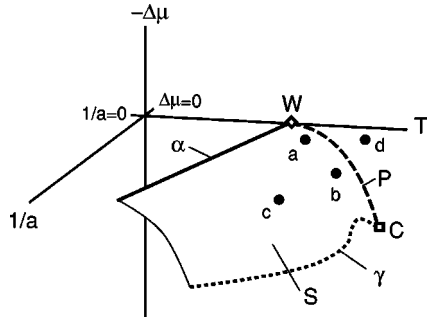

FIG. 3. The thermodynamic states at which the morphological phase transitions take place are located on the surface ''S.'' The lines of coexistence shown as full lines in Fig. 2 are slices through this surface ''S'' at constant values of $1/a$. ''S'' is a surface of first-order transitions and separates the region where the repelled solution is stable (above ''S'') from the region where the bound solution is stable (below ''S''). It is bounded by the prewetting line (dashed line ''P'') which lies in the plane $1/a=0$, by the line γ (dotted line) of critical points of the morphological phase transitions, and by the line α which lies in the plane $\Delta\mu=0$ indicating the loci $(T_0(a),1/a)$ of the morphological phase transitions at bulk liquid-vapor coexistence. ''W'' and ''C'' indicate the first-order wetting transition on a homogeneous ''+'' substrate ($\diamond$) and the prewetting critical point ($\square$), respectively; both lie in the plane $1/a=0$. Indicated by the thin line in the front, ''S'' extends out to larger values of $1/a$ where, however, it is increasingly smeared out by the fluctuation-induced rounding of the morphological phase transition (compare Fig. 2). Due to $T_{pre}(\Delta\mu)-T_t(\Delta\mu;a\to\infty)\sim a^{-1}$, in terms of $1/a$ ''S'' is approximately a ruled surface: one of the two principal curvatures is very small, vanishing exactly in the limit $1/a\to 0$. The thermodynamic states denoted by ''a,'' ''b,'' and ''c'' ($\bullet$, compare Fig. 2) lie on the surface ''S'' whereas the thermodynamic state ''d'' is located above ''S.''

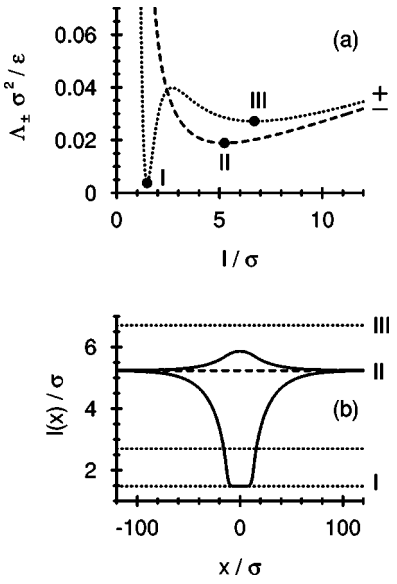

FIG. 4. (a) Effective interface potential Λ_+ of the stripe part (dotted line) and Λ_- of the embedding substrate (dashed line) for the thermodynamic state denoted as ''a'' in Figs. 2 and 3 ($T^*=1.1$, $\Delta\mu^*=0.005$). I, II, and III indicate the local minima of $\Lambda_\pm$. The global minimum of $\Lambda_\pm$ corresponds to the equilibrium film thickness l on a homogeneous ''$\pm$'' substrate. $\Lambda_\pm(l\to\infty)$ increases linearly with the slope $(\rho_l-\rho_g)\Delta\mu$. (b) Equilibrium liquid-vapor interface profiles for the same thermodynamic state as in (a) and for the stripe width $a\approx 27.5\sigma$ for which at this value of T and $\Delta\mu$ the morphological phase transition takes place (see Fig. 3). Therefore the value of the functional $\Omega_{\mathcal{S}}$ is the same for both interface profiles shown here. The dotted (dashed) lines indicate the positions of the extrema of Λ_+ (Λ_-).

calculate the dependence of the effective interface potentials $\Lambda_\pm(l)=\Delta\Omega_b l+\omega_\pm(l)$ on temperature T and undersaturation $\Delta\mu$ from the coefficients ϵ,σ, and $u_i^\pm$ of the interaction potentials and the temperature and undersaturation dependence of the bulk densities ρ_l and ρ_g. Here we use $u_3^+=3.710\epsilon\sigma^3$, $u_4^+=5.566\epsilon\sigma^4$, $u_9^+=0.876\epsilon\sigma^9$, $u_3^-=1.892\epsilon\sigma^3$, $u_4^-=11.355\epsilon\sigma^4$, and $u_9^-=0.252\epsilon\sigma^9$. For this choice of parameters the temperature dependence of $\omega_+(l)$ for the stripe part is such that a homogeneous ''+'' substrate exhibits a first-order wetting transition at $T_w^*=k_BT_w/\epsilon\approx 1.102$ and prewetting transitions along the prewetting line $\Delta\mu_{pre}(T),T>T_w$, and $\Delta\mu>0$, that extends into the vapor phase region of the phase diagram (thick dashed line denoted as ''P'' in Fig. 2). The temperature dependence of $\omega_-(l)$ for the embedding substrate is such that the asymptotic film thickness l_- grows with increasing T and shrinks with increasing $\Delta\mu$. As it turns out, however, the exact temperature dependence and the magnitude of l_- are not important for the qualitative features of the phase diagram for the morphological transitions.

The systems under consideration here differ from those studied in Ref. [12] in two important aspects. First, here the liquidlike films are so thin that they are completely under the influence of the substrate potential which determines, *inter alia*, the effective interface potential. Second, we consider a grand canonical ensemble without a volume constraint for the liquid phase so that the liquidlike films are not subject to instabilities along the y direction as observed in, e.g., Ref. [12].

Using a numerical relaxation technique [13] we solve the two-point boundary value problem for the Euler-Lagrange equation

$$\sigma_{lg}\frac{d^2l(x)}{dx^2}=\Delta\Omega_b+\left.\frac{\partial\omega(x,l)}{\partial l}\right|_{l=l(x)} \quad \text{with} \quad l(x\to\pm\infty)=l_-, \tag{2}$$

which follows from Eq. (1) by functional differentiation with respect to $l(x)$. Equation (2) exhibits the structure of a one-dimensional classical mechanical equation of motion in a time-dependent external potential. With the stripe width a and the temperature T fixed, for a wide range of undersaturations there are two solutions of Eq. (2) which correspond to local minima of the functional $\Omega_{\mathcal{S}}$. One of the solutions is closely bound to the stripe whereas the other solution is further away or even repelled from the stripe as described in Ref. [6]. Figures 4–7 show pertinent examples for the effective potentials $\Lambda_\pm$ of the two substrate materials and the two appertaining solutions of Eq. (2) at three different points of the phase diagram: Figs. 4, 5, 6, and 7 correspond to the points $(T,\Delta\mu)$ indicated by ''a,'' ''b,'' ''c,'' and ''d,'' respectively, in the phase diagram shown in Figs. 2 and 3. The equilibrium solution $\overline{l}(x)$ for the profile corresponds to the global minimum of $\Omega_{\mathcal{S}}$, and the other solution is metastable.

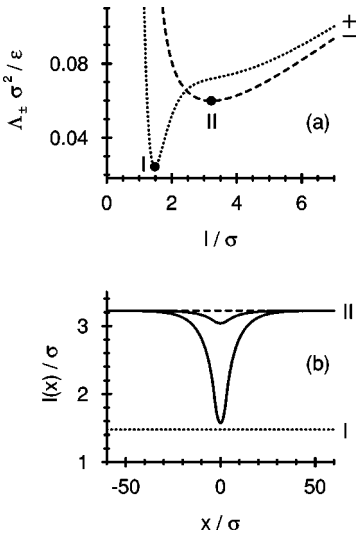

FIG. 5. (a) Same as in Fig. 4(a), but for $T^*=1.1$ and $\Delta\mu^*=0.025$, i.e., for the thermodynamic state denoted as ''b'' in Figs. 2 and 3. The equilibrium interface profiles shown in (b) correspond to $a\approx 6.4\sigma$, for which at the given thermodynamic state the morphological transition takes place (see Fig. 3). In contrast to the situation shown in Fig. 4 the repelled solution is bent towards the substrate and there is only one local minimum (I) of Λ_+.

At a certain value $\Delta\mu_t$, for which Ω_S has the same value for both solutions, a phase transition from one interfacial configuration to the other takes place. This transition is first order because the derivatives of $\Omega_S[\overline{l}(x)]$ with respect to $\Delta\mu$ are discontinuous.

As already shown in Ref. [6], in Eq. (1) the two contributions to Ω_S compete with each other in minimizing the whole functional. Depending on the special choices for a, T, and $\Delta\mu$ the cost in free energy for increasing the liquid-vapor interface area is overcompensated by the gain in free energy which follows from occupying the deeper minimum (I) of Λ_+ near the wall, so that the bound configuration has the lower free energy. In the opposite case this gain in free energy is too small to compensate the cost in free energy from the increased area of the liquid-vapor interface, leading to a less bound or even repelled interface profile.

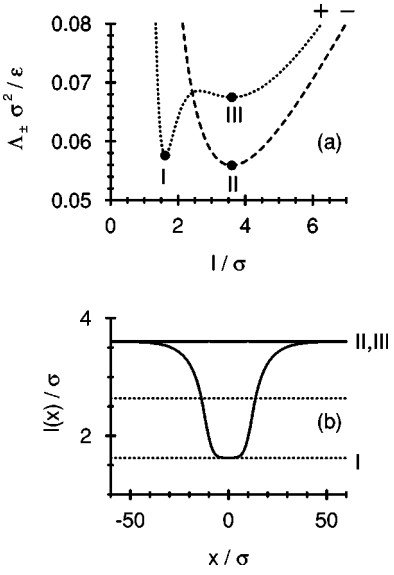

FIG. 6. (a) Same as in Fig. 4(a), but for $T^*=1.155$ and $\Delta\mu^*\approx 0.0232$, i.e., for the thermodynamic state denoted as ''c'' in Figs. 2 and 3 which is located on the line ''ii.'' The equilibrium interface profiles shown in (b) correspond to $a\approx 26\sigma$, for which at the given thermodynamic state the morphological transition takes place (see Fig. 3). The positions of the minima II of Λ_+ and III of Λ_- coincide so that the repelled interface shown in (b) is flat: $l_{rep}(x)\equiv l_-$ where l_- is the position of both minima II and III.

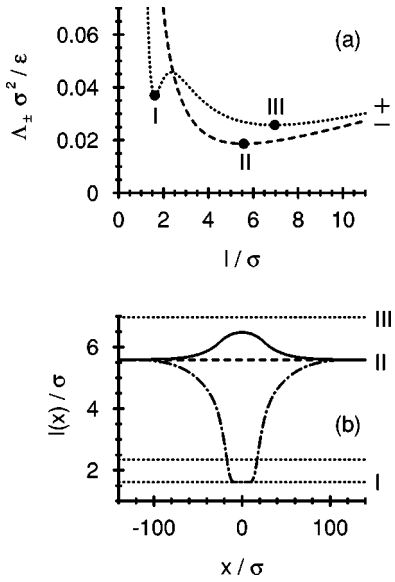

FIG. 7. (a) Same as in Fig. 4(a), but for $T^*=1.15$ and $\Delta\mu^*=0.005$, i.e., for the thermodynamic state denoted as ''d'' in Figs. 2 and 3. (b) Shown are the interface profiles for this state and for $a=50\sigma$. In this case the minimum III of Λ_+ is deeper than the local minimum I because of $T>T_{pre}$. Therefore for all temperatures within the range $T_{pre}(\Delta\mu)<T<T_{iii}(\Delta\mu)$, such as the one chosen here, the repelled solution (full line) is the equilibrium profile (see Fig. 3) whereas the bound solution (dash-dotted line) is metastable. The line $T_{iii}(\Delta\mu)$ is shown as the dotted line ''iii'' in Fig. 2.

III. DISCUSSION OF THE PHASE DIAGRAM

In Fig. 2 the lines $\Delta\mu_t(T;a)=\mu_0(T)-\mu_t(T;a)$ of phase coexistence between the bound and the repelled configuration for different stripe widths a are presented. These lines are vertical cross sections of the full phase diagram shown in Fig. 3. For a given stripe width a the bound (repelled) solution is stable for $-\Delta\mu<-\Delta\mu_t(T;a)$ $(-\Delta\mu>-\Delta\mu_t(T;a))$, i.e., below (above) the corresponding line of phase coexistence. The triangles indicate the intersections $T_0(a)$ between the coexistence lines $\Delta\mu_t(T;a)$ and the bulk liquid-vapor coexistence line $\Delta\mu=0$. At $T_0(a)$ the morphological phase transition occurs at liquid-vapor coexistence, forming the line denoted as α in Fig. 3. Upon increasing the stripe width a the lines of coexistence are shifted towards the prewetting line ''P'' without touching or crossing it for any finite value of a. (This means that for large a the lines of coexistence do not end and reappear at the prewetting line such as, e.g., the prefilling transition lines in a wedge-shaped groove for large opening angles of the wedge [14].) For constant undersaturation $\Delta\mu$ we find $T_{pre}(\Delta\mu)-T_t(\Delta\mu;a\to\infty)\sim a^{-1}$ for the difference between the transition tem-

peratures $T_t(\Delta\mu;a)$ for the morphological and the prewetting transition. In the limit $a\to\infty$ the morphological phase transition tallies with the prewetting transition on the homogeneous ''+'' substrate.

On the mean-field level considered hitherto each coexistence curve $\Delta\mu_t(T;a)$ is a line of first-order transitions ending in a critical point $(T_c(a),\Delta\mu_c(a))$ (denoted as full diamonds in Fig. 2 and forming the line denoted as γ in Fig. 3) such that at $T>T_c(a)$ or $-\Delta\mu<-\Delta\mu_c(a)$, for the given stripe width a there is no morphological transition but a smooth variation from the bound to the repelled solution. As demonstrated by Fig. 2 and its inset the positions of the critical points exhibit a nontrivial and nonmonotonous dependence on the stripe width a; there is no simple criterion for the effective interface potential $\Lambda_\pm$ which allows one to predict the corresponding line of critical points (see the line γ in Fig. 3) as a function of a. As already pointed out in detail in Ref. [6], interface fluctuations along the y direction in this effectively one-dimensional stripe configuration actually smear out the sharp first-order morphological phase transitions and thus eliminate the critical points [15]. In Fig. 2 for $a=5\sigma$ the width of this fluctuation-induced smooth transition region is indicated by the thin dash-dotted lines. For $a\geqslant 10\sigma$ these fluctuation effects are already negligibly small, apart from the close vicinity of the critical points which are still eliminated for any finite a. However, in the limit $a\to\infty$ the coexistence lines $\Delta\mu_t(T;a)$ merge with the prewetting line ''P'' (see Fig. 3) associated with the homogeneous ''+'' substrate, which does have a genuine critical point ''C'' beyond mean-field theory.

The three thermodynamic states denoted as ''a,'' ''b,'' and ''c'' in Figs. 2 and 3 lead to the interface configurations shown in Figs. 4, 5, and 6, respectively. The corresponding effective interface potentials $\Lambda_\pm(l)$ differ with respect to the number and the relative positions of their local minima. For temperatures $T<T_{pre}$ and small undersaturations $\Delta\mu,\Lambda_+(l)$ exhibits two local minima (I and III); an example for this case is shown in Fig. 4 appertaining to the thermodynamic state denoted as ''a'' in Fig. 2. This case is analogous to that described in Ref. [6]. At the thin dotted line $\Delta\mu_i(T)$ denoted as ''i'' in Fig. 2 the minimum III of Λ_+ far from the wall and the maximum of Λ_+ merge, forming a saddle point; $\Delta\mu_i(T)$ ends at the prewetting critical point ''C.'' For $-\Delta\mu\leqslant-\Delta\mu_i(T)$ there is only one local minimum (I) of Λ_+. An example for this latter situation is shown in Fig. 5 corresponding to the thermodynamic state denoted as ''b'' in Fig. 2. Surprisingly the coexistence lines $\Delta\mu_t(T;a)$ for the morphological phase transition extend below this line ''i.'' This shows that the presence of an energy barrier and of a second local minimum of Λ_+ is not a necessary condition for the occurrence of the morphological phase transition described here and in Ref. [6]. The thin dotted line $\Delta\mu_{iii}(T)$ denoted as ''iii'' is the line at which, analogously, the minimum I near the wall and the maximum of Λ_+ merge, forming a saddle point. Both lines ''i'' and ''iii'' meet and end at the critical point ''C'' of the prewetting transition of a homogeneous + substrate where both minima I and III and the maximum of Λ_+ merge, leaving a single minimum.

At the thin short-dashed line $\Delta\mu_{ii}(T)$ denoted as ''ii'' in Fig. 2 the positions of the second minimum III of Λ_+ and of the minimum II of Λ_- coincide. Along this line one of the solutions of Eq. (2) is completely flat: due to $d\Lambda_\pm/dl(l=l_-)=0$ Eq. (2) leads to the trivial solution $l(x)\equiv l_-$ with $d^2l(x)/dx^2\equiv 0$. An example for this case is shown in Fig. 6 which corresponds to the thermodynamic state denoted as ''c'' in Fig. 2. The line ''ii'' separates the region where the repelled solution is bent towards the stripe $(-\Delta\mu<-\Delta\mu_{ii}(T))$ from that where it is bent away from the stripe $(-\Delta\mu>-\Delta\mu_{ii}(T))$. We note that the fact that one of the solutions is completely flat is an artifact of our simplifying model assumption that $\omega(x,l)$ varies steplike as a function of x. In a more realistic model with a smooth lateral variation of the effective interface potential (as used in Ref. [6]) the corresponding solution would be almost flat with a small curvature. In the system considered here the asymptotic film thickness l_-, i.e., the position of minimum II, is always larger than the position of minimum I. However, for low temperatures there is a line at which the minimum II of Λ_- and the *maximum* of Λ_+ coincide. This occurs along the thin long-dashed line $\Delta\mu_{iv}(T)$ denoted as ''iv'' in Fig. 2. This line is the continuation of line ''ii'' for lower temperatures T starting at the point where the line ''ii'' meets the line ''i'' tangentially. Along this line, too, the repelled solution of Eq. (2) is constant, i.e., $l(x)\equiv l_-$. As the line ''ii,'' also line ''iv'' separates two regions with different curvature behavior of the repelled solution.

For temperatures $T>T_{pre}$, i.e., on the right side of the prewetting line P, the minimum III of Λ_+ is deeper than the minimum I. The difference between the asymptotic film thickness l_- corresponding to the minimum II and the deeper minimum III is also smaller than that between l_- and the local minimum I near the wall. Therefore both contributions to Ω_S are larger in the case that the interface follows minimum I as compared to the case that it follows minimum III so that for $T>T_{pre}$ the bound solution is always metastable. This situation is shown in Fig. 7 which corresponds to the thermodynamic state denoted as ''d'' in Fig. 2. If $T\geqslant T_{iii}(\Delta\mu)$ Λ_+ exhibits only one local minimum (III) and therefore there is only one solution of Eq. (2), namely, the repelled one.

IV. CONCLUSION

Within an interface displacement model based on a microscopic density functional theory we have calculated the entire phase diagram (Figs. 2 and 3) of morphological phase transitions of wetting films on a substrate with a chemical stripe (Fig. 1). This phase diagram and the corresponding equilibrium interface profiles shown in Figs. 4–7 elucidate the dependence of the morphological phase transitions on the thermodynamic variables temperature and undersaturation (or, equivalently, pressure) as well as on the stripe width. The morphological phase transitions have been put into the context of the prewetting transitions occurring on a homogeneous substrate formed by particles of the stripe material.

ACKNOWLEDGMENT

We gratefully acknowledge financial support by the German Science Foundation within the Special Research Initiative ''Wetting and Structure Formation at Interfaces.''

[1] Y. Xia and G.M. Whitesides, Annu. Rev. Mater. Sci. **28**, 153 (1998); D.W.L. Tolfree, Rep. Prog. Phys. **61**, 313 (1998); F. Burmeister, C. Schäfle, B. Keilhofer, C. Bechinger, J. Boneberg, and P. Leiderer, Adv. Mater. **10**, 495 (1998).

[2] J.B. Knight, A. Vishwanath, J.P. Brody, and R.H. Austin, Phys. Rev. Lett. **80**, 3863 (1998); M. Grunze, Science **283**, 41 (1999), and references therein; B.H. Weigl and P. Yager, *ibid.* **283**, 346 (1999).

[3] R.F. Service, Science **282**, 399 (1998); M.A. Burns *et al.*, *ibid.* **282**, 484 (1998); H. Shi, W.-B. Tsai, M.D. Garrison, S. Ferrari, and B.D. Ratner, Nature (London) **398**, 593 (1999).

[4] S. Cowan, Chem. Industry **15**, 584 (1999).

[5] S. Dietrich, *Fluids in Contact with Structured Substrates*, Vol. 529 of *NATO Advanced Study Institute, Series C: New Approaches to Problems in Liquid State Theory*, edited by C. Caccamo, J.P. Hansen, and G. Stell (Kluwer, Dordrecht, 1999), p. 197.

[6] C. Bauer, S. Dietrich, and A.O. Parry, Europhys. Lett. **47**, 474 (1999).

[7] S. Dietrich, in *Phase Transitions and Critical Phenomena*, edited by C. Domb and J.L. Lebowitz (Academic, London, 1988), Vol. 12, p. 1.

[8] G. Wiegand, T. Jaworek, G. Wegner, and E. Sackmann, J. Colloid Interface Sci. **196**, 299 (1997).

[9] S. Herminghaus, A. Fery, and D. Reim, Ultramicroscopy **69**, 211 (1997); T. Pompe, A. Fery, and S. Herminghaus, Langmuir **14**, 2585 (1998).

[10] C. Bauer and S. Dietrich, Phys. Rev. E **60**, 6919 (1999).

[11] C. Bauer and S. Dietrich, Eur. Phys. J. B **10**, 767 (1999).

[12] H. Gau, S. Herminghaus, P. Lenz, and R. Lipowsky, Science **283**, 46 (1999).

[13] W.H. Press, S.A. Teukolsky, W.T. Vetterling, and B.P. Flannery, *Numerical Recipes in C*, 2nd ed. (Cambridge University Press, Cambridge, 1992), p. 762 ff.

[14] K. Rejmer, S. Dietrich, and M. Napiórkowski, Phys. Rev. E **60**, 4027 (1999).

[15] V. Privman and M.E. Fisher, J. Stat. Phys. **33**, 385 (1983); J. Appl. Phys. **57**, 3327 (1985); See also M.P. Gelfand and R. Lipowsky, Phys. Rev. B **36**, 8725 (1987); T. Bieker and S. Dietrich, Physica A **252**, 85 (1998); **259**, 466 (1998), and Refs. [5] and [14].